Uncertainty Principle of Interactive Measurements Supplemental Material

Yunlong Xiao,[1,*] Yuxiang Yang,[2,3,†] Ximing Wang,[1] Qing Liu,[1] and Mile Gu[1,4,‡]

[1] *Nanyang Quantum Hub, School of Physical and Mathematical Sciences, Nanyang Technological University, Singapore 637371, Singapore*
[2] *QICI Quantum Information and Computation Initiative, Department of Computer Science, The University of Hong Kong, Pokfulam Road, Hong Kong*
[3] *Institute for Theoretical Physics, ETH Zürich, 8093 Zürich, Switzerland*
[4] *Complexity Institute, Nanyang Technological University, Singapore 639673, Singapore*

(Dated: March 2, 2022)

In this Supplemental Material, we provide more detailed analysis and proofs of the results presented in the main text. Furthermore, a strengthened entropic uncertainty relation has also been offered. For this purpose, some basic knowledge of majorization lattice, including the construction of flatness process, has been supplied. Focusing on the families of maximal common-cause and direct-cause indicators, we develop a fundamental trade-off relation on causal dependencies of quantum dynamics. We demonstrate our results through applications to quantum causal inference. Numerical experiments have also been provided. Finally, it is worth noting that we may reiterate some of the steps in the main text to make the Supplemental Material more explicit and self-contained.

CONTENTS

I. PRELIMINARIES

In this section, we present our notation and prepare the groundwork for our main results. This preparatory work contains four parts: the introduction of Choi-Jamiołkowski (CJ) isomorphism [1, 2] beyond quantum channels, the framework of majorization lattice, the guessing game player between two parties and the universal uncertainty relation for interactive measurements.

* mathxiao123@gmail.com
† yuxiang@cs.hku.hk
‡ mgu@quantumcomplexity.org

A. Choi-Jamiołkowski Isomorphism

Let us start with the concept of Choi operator [1, 2]. For a quantum channel $\mathcal{E}: A \to B$, its Choi operator $J^{\mathcal{E}}_{AB}$ is defined as

$$J^{\mathcal{E}}_{AB} := \mathrm{id}_A \otimes \mathcal{E}_{A' \to B}(|I\rangle\langle I|_{AA'}), \tag{1}$$

where $|I\rangle_{AA'} := \sum_i |i\rangle_A |i\rangle_{A'}$ is the unnormalized maximally entangled state with A' being a replica of system A, and $\{|i\rangle\}$ being an orthonormal basis on A. Here the correspondence between quantum channel $\mathcal{E}$ and its Choi operator $J^{\mathcal{E}}$ is referred as the Choi-Jamiołkowski isomorphism in quantum information theory [3–5]. Note that $\mathcal{E}$ is (i) completely positive (CP) if and only if its Choi operator satisfies $J^{\mathcal{E}} \geqslant 0$ and (ii) trace-preserving (TP) if and only if its Choi operator satisfies $\mathrm{Tr}_B[J^{\mathcal{E}}_{AB}] = \mathbb{1}_A$.

When investigating complex quantum dynamics, constituting of sequential quantum channels, it is necessary to understand the correlation between the Choi operator of its components and the whole quantum dynamics. Let us consider a concrete example, assume a quantum channel $\mathcal{E}_1 : A \to BE$ is followed by another one $\mathcal{E}_2 : CE \to D$, and connected through the quantum memory E. Then the whole quantum dynamics $\mathcal{E} := \mathcal{E}_2 \circ \mathcal{E}_1$ is a linear map from AC to BD, satisfying the following conditions:

(i) CP,

(ii) TP,

(iii) non-signaling (NS) from $C \to D$ to $A \to B$.

Denote the Choi operator of $\mathcal{E}_1$ and $\mathcal{E}_2$ as J^1_{ABE} and J^2_{CDE} (or simply J^1 and J^2) respectively, then it is straightforward to check that the Choi operator of $\mathcal{E}_2 \circ \mathcal{E}_1$ is given by $\mathrm{Tr}_E[(J^1)^{\mathbf{T}_E} \cdot J^2]$, which motivates the developments of *link product* $\star$ [6, 7].

Mathematically, given two operators M and N acting on spaces XY and YZ, we define their link product $M \star N$ as $M \star N := \mathrm{Tr}_Y[M^{\mathbf{T}_Y} \cdot N]$, where the common space Y is appeared as the link between M and N and has been "swallowed" by the product. Equipped with the link product, now we can rewrite the Choi operator of $\mathcal{E} = \mathcal{E}_2 \circ \mathcal{E}_1$ as

$$J^{\mathcal{E}} = J^1 \star J^2. \tag{2}$$

Here $\mathcal{E} = \mathcal{E}_2 \circ \mathcal{E}_1$ is a typical example of quantum superchannel, with channels $\mathcal{E}_1$ and $\mathcal{E}_2$ be the pre-processing and post-processing of $\mathcal{E}$.

Similar to the case of quantum channels, all above restrictions can be translated into the language of Choi operator; a map $\mathcal{E}$ from AC to BD is (i) CP if and only if $J^{\mathcal{E}} \geqslant 0$, (ii) TP if and only if $\mathrm{Tr}_{BD}[J^{\mathcal{E}}] = \mathbb{1}_{AC}$, and (iii) NS from $C \to D$ to $A \to B$ if and only if $\mathrm{Tr}_D[J^{\mathcal{E}}] = \mathrm{Tr}_{CD}[J^{\mathcal{E}}] \otimes \mathbb{1}_C/d_C$ with $d_C := \dim C$.

Based on above discussion, it is clear that the quantum dynamics $\Phi_{B\to AC}$ (see Fig. 2 of our main text) discussed in our main text forms a special case of quantum superchannel, with trivial input system of pre-processing. This means that all the physical evolution before our intervention has been encoded into a process of state preparation. Thanks to the main result of Ref. [8], we know that any superchannel, including $\Phi_{B\to AC}$, can be divided into two quantum processes: pre-processing and post-processing. Here we denote the pre- and post- processing of $\Phi_{B\to AC}$ as $\Psi^{\mathrm{Pre}}_{\mathbb{C}\to AE}$ and $\Psi^{\mathrm{Post}}_{BE\to C}$ respectively, namely

$$\Phi_{B\to AC} = \Psi^{\mathrm{Post}}_{BE\to C} \circ \Psi^{\mathrm{Pre}}_{\mathbb{C}\to AE}. \tag{3}$$

The Choi operator of $\Phi_{B\to AC}$ can be evaluated explicitly based on the Choi operators of $\Psi^{\mathrm{Pre}}_{\mathbb{C}\to AE}$ and $\Psi^{\mathrm{Post}}_{BE\to C}$, denoted as J^{Pre} and J^{Post}. That is

$$J^{\Phi} = J^{\mathrm{Pre}} \star J^{\mathrm{Post}}. \tag{4}$$

Here J^{Φ} acting on systems ABC satisfies CPTP and NS from $B \to C$ to A:

(i) CP $\quad J^{\Phi} \geqslant 0$,

(ii) TP $\quad \mathrm{Tr}_{AC}[J^{\Phi}] = \mathbb{1}_B$,

(iii) NS from $B \to C$ to A $\quad \mathrm{Tr}_C[J^{\Phi}] = \mathrm{Tr}_{BC}[J^{\Phi}] \otimes \mathbb{1}_B/d_B$.

Actually, these conditions can be further simplified as $J^{\Phi} \geqslant 0$ and $\mathrm{Tr}_C[J^{\Phi}] = \rho_A \otimes \mathbb{1}_B$ for some quantum state ρ_A.

From an experimental viewpoint, the Choi state of $\Phi_{B\to AC}/d_B$ can be obtained directly by considering the following map

$$\mathrm{id}_B \otimes \Phi_{B'\to AC}(\phi^{+}_{BB'}), \tag{5}$$

where $\phi^{+}_{BB'} := |I\rangle\langle I|_{BB'}/d_B$ with $|I\rangle_{BB'} := \sum_i |i\rangle_B |i\rangle_{B'}$ be the unnormalized maximally entangled state with $B^{'}$ being a replica of system B, and $\{|i\rangle\}$ being an orthonormal basis on B, as demonstrated in Fig. 1.

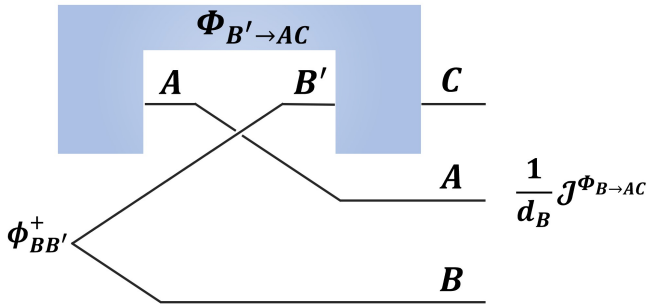

FIG. 1: (color online) Circuit realization of the Choi operator $J^{\Phi_{B\to AC}}$, where $\phi^{+}_{BB'} := |I\rangle\langle I|_{BB'}/d_B$ stands for the maximally entangled state on systems $BB^{'}$.

We now move on to investigating the Choi operator of an interactive measurement for quantum dynamics $\Phi_{B\to AC}$. Assume such an interactive measurement $\mathcal{T}$ consists of a quantum channel Λ from system A to BR, a bipartite POVM $M := \{M_x\}_x$ acting on systems CR, and an ancillary system R connecting them together (see Fig. 2a of our main text):

$$\mathcal{T}_{AC\to B\mathbb{C}} := \{M_x \circ \Lambda_{A\to BR}\}_x. \tag{6}$$

Then each $\mathcal{T}_x := M_x \circ \Lambda_{A\to BR}$ forms a CP and trace-non-increasing (TNI) map from AC to B. Since the Choi operator of the positive operator-valued measure (POVM) M_x is given by $M_x^{\mathbf{T}_{CR}}$, we have that the Choi operator of $\mathcal{T}_x$, denoted as J_x, is characterized by

$$J_x = M_x^{\mathbf{T}_{CR}} \star J^{\Lambda}. \tag{7}$$

To realize the Choi state $J_x/d_A d_C$ experimentally, we employ the quantum circuit shown in Fig. 2. For any incompatible measuring processes $\mathcal{T}_1 = \{J_x^{\mathcal{T}_1}\}_{x=1}^m$ and $\mathcal{T}_2 = \{J_y^{\mathcal{T}_2}\}_{y=1}^n$ specified by

$$J_x^{\mathcal{T}_1} = M_x^{\mathbf{T}_{CR}} \star J^{\Lambda_{A\to BR}}, \tag{8}$$

$$J_y^{\mathcal{T}_2} = N_y^{\mathbf{T}_{CR}} \star J^{\Upsilon_{A\to BR}}, \tag{9}$$

the probability of obtain classical outcomes x and y from quantum dynamics $\Phi_{B\to AC} = \Psi^{\mathrm{Post}}_{BE\to C} \circ \Psi^{\mathrm{Pre}}_{\mathbb{C}\to AE}$ is given by

$$p_x = \mathrm{Tr}\big[M_x \cdot \Psi^{\mathrm{Post}}_{BE\to C} \circ \Lambda_{A\to BR}(\Psi^{\mathrm{Pre}}_{\mathbb{C}\to AE})\big], \tag{10}$$

$$q_y = \mathrm{Tr}\big[N_y \cdot \Psi^{\mathrm{Post}}_{BE\to C} \circ \Upsilon_{A\to BR}(\Psi^{\mathrm{Pre}}_{\mathbb{C}\to AE})\big]. \tag{11}$$

By using Choi operators, they can also be rewritten as

$$p_x = J^{\Phi} \star J_x^{\mathcal{T}_1}, \tag{12}$$

$$q_y = J^{\Phi} \star J_y^{\mathcal{T}_2}, \tag{13}$$

where J^{Φ} stands for the Choi operator of quantum dynamics $\Phi_{B\to AC}$. If the quantum dynamics Φ satisfies $J^{\Phi} \star J_x^{\mathcal{T}_1} = 1$ for some x, then we call Φ an *eigencircuit* of interactive measurement $\mathcal{T}_1$. Similarly, when $J^{\Phi} \star J_y^{\mathcal{T}_2} = 1$ for some y, we call the quantum dynamics Φ an eigencircuit of interactive measurement $\mathcal{T}_2$. Collect p_x and q_y into two probability vector $\mathbf{p}$ and $\mathbf{q}$, namely $\mathbf{p} := \{p_x\}_{x=1}^m$ and $\mathbf{q} := \{q_y\}_{y=1}^n$. Till now, we have transformed the original problem related with quantum dynamics $\Phi_{B\to AC}$ to the probability vectors $\mathbf{p}$ and $\mathbf{q}$. However, it is still not enough to derive the entropic uncertainty relation presented in our main text. A useful tool known as flatness process – originally introduced to investigate the supermodularity and subadditivity of entropies [9] – that deals with the probability vectors is needed.

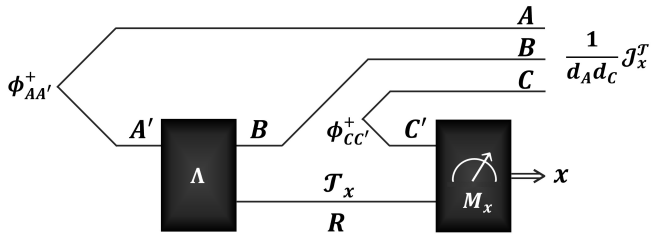

FIG. 2: (color online) Circuit realization of the Choi operator J_x, where $\phi^+_{AA'} := |I\rangle\langle I|_{AA'}/d_A$ and $\phi^+_{CC'} := |I\rangle\langle I|_{CC'}/d_C$ stand for the maximally entangled states on systems $AA^{'}$ and $CC^{'}$ respectively.

B. Majorization Lattice

In this subsection we turn our attention to the concept of lattice, which will be useful for constructing the optimal bound for *universal uncertainty relation* investigated in next subsection. Let us start with the definition of *Lattice*: A quadruple $(S, \sqsubset, \wedge, \vee)$ is called lattice if $\sqsubset$ is a partial oder on the set S such that for all $\mathbf{p}$, $\mathbf{q} \in S$ there exists a unique greatest lower bound (GLB) $\mathbf{p} \wedge \mathbf{q}$ and a unique least upper bound (LUB) $\mathbf{p} \vee \mathbf{q}$ satisfying

$$\begin{aligned} &\mathbf{x} \sqsubset \mathbf{p},\, \mathbf{x} \sqsubset \mathbf{q} \Rightarrow \mathbf{x} \sqsubset \mathbf{p} \wedge \mathbf{q}, \\ &\mathbf{p} \sqsubset \mathbf{y},\, \mathbf{q} \sqsubset \mathbf{y} \Rightarrow \mathbf{p} \vee \mathbf{q} \sqsubset \mathbf{y}. \end{aligned} \tag{14}$$

for each $\mathbf{x}$, $\mathbf{y} \in S$. A special class of lattices are those which have GLB and LUB for all their subsets, namely *Complete Lattice*: A lattice $(S, \sqsubset, \wedge, \vee)$ is called complete, if for any nonempty subset $R \subset S$, it has a LUB, denoted by $\vee R$ and a GLB, denoted by $\wedge R$. More precisely, if $\mathbf{x}, \mathbf{y} \in S$ such that $\mathbf{x} \sqsubset R \sqsubset \mathbf{y}$, i.e.

$$\mathbf{x} \sqsubset \mathbf{p} \sqsubset \mathbf{y}, \quad \forall \mathbf{p} \in R, \tag{15}$$

we thus have

$$\mathbf{x} \sqsubset \wedge R \quad \text{and} \quad \vee R \sqsubset \mathbf{y}. \tag{16}$$

Here we use the notation "$\prec$" to denote the majorization [10]: For vectors $\mathbf{x} = (x_k)_k$, $\mathbf{y} = (y_k)_k \in \mathbb{R}^d$, we have $\mathbf{x} \prec \mathbf{y}$ whenever $\sum_{k=1}^i x_k^{\downarrow} \leqslant \sum_{k=1}^i y_k^{\downarrow}$ for all $1 \leqslant i \leqslant d-1$ and $\sum_{k=1}^d x_k = \sum_{k=1}^d y_k$, where the downarrow notation $^{\downarrow}$ means the components of corresponding vector are arranged in non-increasing order. For example, any 3-dimensional probability vector $\mathbf{p}$ satisfies $(1/3, 1/3, 1/3) \prec \mathbf{p} \prec (1, 0, 0)$. A useful fact about majorization is that, the set $\mathbb{P}_n^{d,\downarrow} := \{\mathbf{x} \in \mathbb{R}^d \,\|\, x_k \geqslant x_{k+1} \geqslant 0, \forall 1 \leqslant k \leqslant d-1, \sum_k x_k = n\}$ forms a complete lattice under majorization [11], called majorization lattice.

The properties of majorization lattice lead to a standard approach in finding the optimal bounds for a subset S of $\mathbb{P}_n^{d,\downarrow}$ [11]. Formally, let us consider $S \subset \mathbb{P}_n^{d,\downarrow}$, and then there are two steps in constructing its LUB $\vee S$. The first step is to find the quantities b_k, which is defined as

$$b_k := \left(\max_{\mathbf{x} \in S} \sum_{i=1}^{k} x_i \right) - \sum_{i=1}^{k-1} b_i, \tag{17}$$

for $1 \leqslant k \leqslant d$. Remark that the vector $\mathbf{b}_S := (b_k)_k$ might not always belongs to the set $\mathbb{P}_n^{d,\downarrow}$. To give our reader some intuition, we recall the example constructed in Ref. [9]. Take $S = \{\mathbf{x}, \mathbf{y}\}$ with

$$\mathbf{x} = (0.6, 0.15, 0.15, 0.1), \tag{18}$$

$$\mathbf{y} = (0.5, 0.25, 0.2, 0.05). \tag{19}$$

In this case, the vector

$$\mathbf{b}_S = (0.6, 0.15, 0.2, 0.05), \tag{20}$$

obtained from (17) does not belong to the set $\mathbb{P}_1^{d,\downarrow}$, since $b_2 = 0.15 < b_3 = 0.2$. Actually, even though we rearrange the vector $\mathbf{b}_S$ into non-increasing order

$$\mathbf{b}_S^{\downarrow} = (0.6, 0.2, 0.15, 0.05), \tag{21}$$

$\mathbf{b}_S^{\downarrow}$ is not the optimal upper bound, i.e. $\mathbf{b}_S^{\downarrow} \neq \vee S$. In order to achieve the optimal bound $\vee S$, an additional manipulation $\mathcal{F}$ on $\mathbf{b}_S$ (not $\mathbf{b}_S^{\downarrow}$) is needed, named *flatness process* [9]: Let $\mathbf{x} \in \mathbb{R}_+^d$ be a vector, and j be the smallest integer in $\{2, \ldots, d\}$ such that $x_j > x_{j-1}$, and i be the greatest integer in $\{1, \ldots, j-1\}$ such that $x_{i-1} \geqslant (\sum_{k=i}^{j} x_k)/(j-i+1) := a$. Define

$$\mathcal{T}(\mathbf{x}) := (x_1', \ldots, x_n') \quad \text{with} \quad x_k' = \begin{cases} a & \text{for} \quad k = i, \ldots, j \\ x_k & \text{otherwise.} \end{cases} \tag{22}$$

and $\mathcal{F}(\mathbf{x}) := \mathcal{T}^{d-1}(\mathbf{x}) = \mathcal{T}(\mathcal{T}^{d-2}(\mathbf{x}))$, i.e. applying $\mathcal{T}$ on the vector $\mathbf{x}$ successively $d-1$ times. Here we call $\mathcal{F}$ the flatness process of vector $\mathbf{x}$. Thanks to flatness process $\mathcal{F}$, we have

$$\vee S = \mathbf{x} \vee \mathbf{y} = \mathcal{F}(\mathbf{b}_S) = (0.6, 0.175, 0.175, 0.05), \tag{23}$$

with

$$(0.6, 0.15, 0.15, 0.1) \prec (0.6, 0.175, 0.175, 0.05) \prec (0.6, 0.15, 0.2, 0.05), \tag{24}$$

$$(0.5, 0.25, 0.2, 0.05) \prec (0.6, 0.175, 0.175, 0.05) \prec (0.6, 0.15, 0.2, 0.05), \tag{25}$$

and for any probability vector $\mathbf{z}$ satisfying $\mathbf{x} \prec \mathbf{z}$ and $\mathbf{y} \prec \mathbf{z}$, it follows that

$$(0.6, 0.175, 0.175, 0.05) \prec \mathbf{z}. \tag{26}$$

It is worth mentioning that the flatness process $\mathcal{F}$ introduced in Ref. [9] is exactly the second step of formulating the optimal bound for S. More precisely, $\vee S = \mathcal{F}(\mathbf{b}_S)$ holds in general [11].

To summarize, the standard approach in finding the optimal bounds for a subset S of $\mathbb{P}_n^{d,\downarrow}$ contains two steps:

Step 1. Formulating $\mathbf{b}_S$ defined in Eq. (17),

Step 2. Applying the flatness process defined in Eq. (22) to obtain $\mathcal{F}(\mathbf{b}_S)$.

C. Guessing Game

Recall the guessing game considered in the main text of our work. In particular, Alice is an agent that is capable of proving its supplied dynamical processes with two possible interactive measurements, $\mathcal{T}_1$ and $\mathcal{T}_2$. Meanwhile, another agent Bob can engineer various dynamical process for Alice to probe. In each round, Alice would select one of the two interactive measurements at random to probe whatever Φ Bob supplies. Alice then announces a tuple (b, x), where $b \in \{1, 2\}$ denotes her choice of interactive measurements, and $x \in \{1, \ldots, m_b\}$ represents the corresponding measurement outcome. Here we assume that $m_1 = m$ and $m_2 = n$. In general, they do not need to be equal. Bob is tasked to place bets on k possible values of (b, x), and he wins if Alice's announcement lands on one of these values. Bob can improve his chances by engineer Φ to his best advantage.

For simplicity purposes, in this subsection, let us investigate the case where Alice's interactive measurements are given by Eq. (8) and (9). On the other hand, Bob's quantum dynamics is a map from B to AC, which is known as causal map in Ref. [12, 13]. If Bob prepares the quantum dynamics $\Phi_{B\to AC}^{\bullet}$, then his successful probability of guessing k outcomes correctly is upper-bounded by

$$\Omega_k(\Phi_{B\to AC}^{\bullet}) := \max_{|\mathcal{S}_1|+|\mathcal{S}_2|=k} \sum_{\substack{x\in\mathcal{S}_1\subset\{1,\ldots,m\} \\ y\in\mathcal{S}_2\subset\{1,\ldots,n\}}} (\frac{1}{2} J_x^{\mathcal{T}_1} + \frac{1}{2} J_y^{\mathcal{T}_2}) \star J^{\Phi_{B\to AC}^{\bullet}} \tag{27}$$

$$= \frac{1}{2} \max_{|\mathcal{S}_1|+|\mathcal{S}_2|=k} \sum_{\substack{x\in\mathcal{S}_1\subset\{1,\ldots,m\} \\ y\in\mathcal{S}_2\subset\{1,\ldots,n\}}} \mathrm{Tr}\Big[(J_x^{\mathcal{T}_1} + J_y^{\mathcal{T}_2}) \cdot (J^{\Phi_{B\to AC}^{\bullet}})^{\mathbf{T}}\Big]. \tag{28}$$

Here $\mathbf{T}$ is the transposition over all systems. Next, we take the union of $J_x^{\mathcal{T}_1}$ and $J_y^{\mathcal{T}_2}$, and denote it by $\{J_z\}_z$, where $J_z = J_z^{\mathcal{T}_1}$ for $1 \leqslant z \leqslant m$ and $J_z = J_{z-m}^{\mathcal{T}_2}$ for $m+1 \leqslant z \leqslant m+n$. We adopt the convention $J_{\mathcal{S}}$ for $\sum_{z\in\mathcal{S}} J_z$, where $\mathcal{S} \subset \{1, \ldots, m+n\}$. Then (27) can be simplified to

$$\Omega_k(\Phi_{B\to AC}^{\bullet}) = \frac{1}{2} \max_{|\mathcal{S}|=k} \sum_{z\in\mathcal{S}} \mathrm{Tr}\Big[J_z \cdot (J^{\Phi_{B\to AC}^{\bullet}})^{\mathbf{T}}\Big] = \frac{1}{2} \max_{|\mathcal{S}|=k} \mathrm{Tr}\Big[J_{\mathcal{S}} \cdot (J^{\Phi_{B\to AC}^{\bullet}})^{\mathbf{T}}\Big]. \tag{29}$$

Assume that Bob can prepare all quantum dynamics, then his greatest successful probability Ω_k of guessing k outcomes correctly is exactly characterized by

$$\begin{aligned}\Omega_k = \frac{1}{2}\max_{|\mathcal{S}|=k}\max \quad & \mathrm{Tr}\big[J_{\mathcal{S}}\cdot J^{\mathbf{T}}\big] \\ \text{s.t.} \quad & J\geqslant 0, \quad \mathrm{Tr}_{AC}[J]=\mathbb{1}_B, \\ & \mathrm{Tr}_C[J]=\mathrm{Tr}_{BC}[J]\otimes\mathbb{1}_B/d_B,\end{aligned} \tag{30}$$

since the Choi operator of $\Phi_{B\to AC}$ satisfies the requirements of (i) CP: $J^{\Phi}\geqslant 0$, (ii) TP: $\mathrm{Tr}_{AC}[J^{\Phi}]=\mathbb{1}_B$ and (iii) NS from $B\to C$ to A: $\mathrm{Tr}_C[J^{\Phi}]=\mathrm{Tr}_{BC}[J^{\Phi}]\otimes\mathbb{1}_B/d_B$. Note that the constraints appeared in (30) remain unchanged if we apply the transpose $\mathbf{T}$ to all systems. Thus, (30) is equivalent to the following optimization problem

$$\begin{aligned}\Omega_k = \frac{1}{2}\max_{|\mathcal{S}|=k}\max \quad & \mathrm{Tr}[J_{\mathcal{S}}\cdot J] \\ \text{s.t.} \quad & J\geqslant 0, \quad \mathrm{Tr}_{AC}[J]=\mathbb{1}_B, \\ & \mathrm{Tr}_C[J]=\mathrm{Tr}_{BC}[J]\otimes\mathbb{1}_B/d_B.\end{aligned} \tag{31}$$

As discussed in Sec. I A, Ω_k can be further simplified as

$$\begin{aligned}\Omega_k = \frac{1}{2}\max_{|\mathcal{S}|=k}\max \quad & \mathrm{Tr}[J_{\mathcal{S}}\cdot J] \\ \text{s.t.} \quad & J\geqslant 0, \quad \mathrm{Tr}[\rho_A]=1, \quad \mathrm{Tr}_C[J]=\rho_A\otimes\mathbb{1}_B.\end{aligned} \tag{32}$$

D. Universal Uncertainty Relation

In this subsection we give a complete characterization of $\mathbf{p}\oplus\mathbf{q}$ considered in (10) and (11), and provide a vector-type bound $\mathbf{v}$ for $\mathbf{p}\oplus\mathbf{q}$

$$\mathbf{p}\oplus\mathbf{q}\prec\mathbf{v}, \tag{33}$$

where $\mathbf{v}$ is state-independent and relies only on the Interactive measurements $\mathcal{T}_1$ and $\mathcal{T}_2$.

From Eq. 32, it is straightforward to obtain the following lemma.

Lemma. *Let us define the probability vector* $\mathbf{w}_{\mathcal{T}_1,\mathcal{T}_2}$ *as*

$$\mathbf{w}_{\mathcal{T}_1,\mathcal{T}_2}:=(\Omega_1,\Omega_2-\Omega_1,\ldots,\Omega_{m+n}-\Omega_{m+n-1}). \tag{34}$$

Then for any quantum dynamics $\Phi_{B\to AC}$ *and two arbitrary* $\mathcal{T}_1$, $\mathcal{T}_2$ *considered in (8) and (9), the induced probability vectors* $\mathbf{p}$ *and* $\mathbf{q}$ *satisfies*

$$\frac{1}{2}\mathbf{p}\oplus\frac{1}{2}\mathbf{q}\prec\mathbf{w}_{\mathcal{T}_1,\mathcal{T}_2}, \tag{35}$$

where $\mathbf{w}_{\mathcal{T}_1,\mathcal{T}_2}$ *depends only on* $\mathcal{T}_1$ *and* $\mathcal{T}_2$.

Denote the set of all possible $\frac{1}{2}\mathbf{p}\oplus\frac{1}{2}\mathbf{q}$ as $S_{\oplus}$, then from the viewpoint of majorization lattice,

$$\mathbf{b}_{S_{\oplus}}=\mathbf{w}_{\mathcal{T}_1,\mathcal{T}_2}. \tag{36}$$

Thus, we have

$$\vee S_{\oplus}=\mathcal{F}(\mathbf{b}_{S_{\oplus}})=\mathcal{F}(\mathbf{w}_{\mathcal{T}_1,\mathcal{T}_2}), \tag{37}$$

which leads to the optimal universal uncertainty relation

$$\frac{1}{2}\mathbf{p}\oplus\frac{1}{2}\mathbf{q}\prec\mathcal{F}(\mathbf{w}_{\mathcal{T}_1,\mathcal{T}_2}). \tag{38}$$

Here "optimal" means that for any vector $\mathbf{z}$ satisfying $\frac{1}{2}\mathbf{p}\oplus\frac{1}{2}\mathbf{q}\prec\mathbf{z}$, we immediately have $\mathcal{F}(\mathbf{w}_{\mathcal{T}_1,\mathcal{T}_2})\prec\mathbf{z}$. Remark that, Eq. (37) is equivalent to

$$\mathbf{p}\oplus\mathbf{q}\prec 2\,\mathcal{F}(\mathbf{w}_{\mathcal{T}_1,\mathcal{T}_2})=\mathcal{F}(2\,\mathbf{w}_{\mathcal{T}_1,\mathcal{T}_2}). \tag{39}$$

Hence, we can take $\mathbf{v}$ as $\mathcal{F}(2\,\mathbf{w}_{\mathcal{T}_1,\mathcal{T}_2})$, which implies that $\mathbf{p}\oplus\mathbf{q}\prec\mathbf{v}$. Now we have finished all the preparation works.

II. ENTROPIC UNCERTAINTY RELATIONS

In this section, we prove the theorem of our main text and offer an improved entropic uncertainty relation based on flatness process. The entropic uncertainty relation for multiple interactive measurements has also been provided.

A. Entropic Uncertainty Relation for Causal Maps

To formulate the direct cause and common cause entropic uncertainty relation, we need to obtain the entropic uncertainty relation for causal maps (such as $\Phi_{B\to AC}$) first.

The class of functions that preserve the "order" of majorization are the Schur-concave functions; that is for any Schur-concave function f and $\mathbf{x} \prec \mathbf{y}$ we have $f(\mathbf{x}) \geqslant f(\mathbf{y})$ [10]. Remarkably, the Rényi entropies, including the Shannon entropy, are Schur-concave function. Hence, by taking f as the Shannon entropy H, we immediately arrive at the following theorem for causal maps.

Theorem 1. *For any causal map $\Phi_{B\to AC}$ and interactive measurements $\mathcal{T}_1$, $\mathcal{T}_2$ considered in (8) and (9), the induced probability vectors* $\mathbf{p}$ *and* $\mathbf{q}$ *satisfies*

$$H(\mathbf{p}) + H(\mathbf{q}) \geqslant 2\, H(\mathbf{w}_{\mathcal{T}_1,\mathcal{T}_2}) - 2 = H(2\,\mathbf{w}_{\mathcal{T}_1,\mathcal{T}_2}). \tag{40}$$

Here we have used the fact that $H(\mathbf{p}\oplus\mathbf{q}) = H(\mathbf{p}) + H(\mathbf{q})$. Remark that when the causal map degenerate to the case of quantum channels, we can simply adopt the framework introduced in [11] to construct $C(\mathcal{T}_1, \mathcal{T}_2)$, which includes a Maassen-Uffink type uncertainty relation. In such case, however, the intervention between quantum dynamics and measurement is absent.

B. Improved Entropic Uncertainty Relation for Causal Maps

From the optimality of $\mathcal{F}(\mathbf{w}_{\mathcal{T}_1,\mathcal{T}_2})$ for the set $S_\oplus$, we have the following inequality chain under majorization

$$\mathbf{p}\oplus\mathbf{q} \prec \mathcal{F}(2\,\mathbf{w}_{\mathcal{T}_1,\mathcal{T}_2}) \prec 2\,\mathbf{w}_{\mathcal{T}_1,\mathcal{T}_2}, \tag{41}$$

which implies that

$$H(\mathbf{p}) + H(\mathbf{q}) \geqslant 2H(\mathcal{F}(\mathbf{w}_{\mathcal{T}_1,\mathcal{T}_2})) - 2 \geqslant 2H(\mathbf{w}_{\mathcal{T}_1,\mathcal{T}_2}) - 2. \tag{42}$$

Consequently, the bound $2H(\mathcal{F}(\mathbf{w}_{\mathcal{T}_1,\mathcal{T}_2})) - 2$ improves the Thm. 1 presented in Sec. II A.

C. Uncertainty Principle of Multiple Interactive Measurements

In this subsection we provide a generalized entropic uncertainty relation for multiple interactive measurements. Assume we can make a interventions on quantum dynamics, and denote the system before and after i-th intervention as A_{2i-1} and A_{2i} respectively. The final system of quantum dynamics is referred as A_{2a+1}. Noted that in this subsection the notation is slightly different from the one presented in our main text. Here we consider a interventions and in the main text we study the case with $a-1$ interventions.

Now the quantum dynamics Φ is a map from $\otimes_{i=1}^{a}\mathcal{H}_{2i}$ to $\otimes_{i=1}^{a+1}\mathcal{H}_{2i-1}$. Mathematically, the Choi operator of Φ forms a "comb" [6, 7]. Without loss of generality, let us assume

$$\Phi := \Psi^{a+1}_{\mathcal{H}_{2a}E_a\to\mathcal{H}_{2a+1}} \circ \cdots \circ \Psi^{2}_{\mathcal{H}_2E_1\to\mathcal{H}_3E_2} \circ \Psi^{1}_{\mathbb{C}\to\mathcal{H}_1E_1} \tag{43}$$

On the other hand, assume we have b interactive measurements $\mathcal{T}_1, \ldots, \mathcal{T}_b$. Each of them is constituted of a quantum channels, followed by a POVM; that is

$$\mathcal{T}_j := \{M_{x_j} \circ \Lambda^{j,a}_{\mathcal{H}_{2a-1}R_{a-1}\to\mathcal{H}_{2a}R_a} \circ \cdots \circ \Lambda^{j,2}_{\mathcal{H}_3R_1\to\mathcal{H}_4R_2} \circ \Lambda^{j,1}_{\mathcal{H}_1\to\mathcal{H}_2R_1}\}_{x_j=1}^{m_j}, \quad j\in\{1,\ldots,b\}. \tag{44}$$

Then the probability of obtaining classical outcome x_j from $\mathcal{T}_j$ is determined by

$$p_{x_j} = \mathrm{Tr}\Big[M_{x_j}\cdot \Psi^{a+1}_{\mathcal{H}_{2a}E_a\to\mathcal{H}_{2a+1}} \circ \Lambda^{j,a}_{\mathcal{H}_{2a-1}R_{a-1}\to\mathcal{H}_{2a}R_a} \circ \cdots \circ \Psi^{2}_{\mathcal{H}_2E_1\to\mathcal{H}_3E_2} \circ \Lambda^{j,1}_{\mathcal{H}_1\to\mathcal{H}_2R_1} \circ \Psi^{1}_{\mathbb{C}\to\mathcal{H}_1E_1}\Big]. \tag{45}$$

Denote the Choi operator of $M_{x_j}\circ\Lambda^{j,a}_{\mathcal{H}_{2a-1}R_{a-1}\to\mathcal{H}_{2a}R_a}\circ\cdots\circ\Lambda^{j,2}_{\mathcal{H}_3R_1\to\mathcal{H}_4R_2}\circ\Lambda^{j,1}_{\mathcal{H}_1\to\mathcal{H}_2R_1}$ and Φ as $J^j_{x_j}$ and J^Φ respectively, then (45) can be re-expressed as

$$p_{x_j}=J^j_{x_j}\star J^\Phi. \tag{46}$$

Collect p_{x_j} into probability vector $\mathbf{p}_j$, and define $J_z:=J^j_{z-\sum_{i=1}^j m_i}$ for $\sum_{i=1}^j m_i+1\leqslant z\leqslant\sum_{i=1}^{j+1}m_i$, $J_{\mathcal{S}}:=\sum_{z\in\mathcal{S}}J_z$, where $\mathcal{S}\subset\{1,\ldots,\sum_{i=1}^b m_i\}$. With these notions, we construct the probability vector $\mathbf{w}_{\mathcal{T}_1,\ldots,\mathcal{T}_b}$ as

$$\mathbf{w}_{\mathcal{T}_1,\ldots,\mathcal{T}_b}:=(\Gamma_{k+1}-\Gamma_k)_{k=0}^{\sum_{i=1}^b m_i}, \tag{47}$$

where $\Gamma_0:=0$ and Γ_k is defined as the solution to the following optimization problem [14, 15]

$$\Gamma_k=\max_{\mathcal{S}:|\mathcal{S}|=k}\quad\gamma_{\mathcal{S}} \tag{48}$$

$$\begin{aligned}\gamma_{\mathcal{S}}:=\max\quad&\mathrm{Tr}[J(a+1)\cdot J_{\mathcal{S}}]/b\\ \text{s.t.}\quad&J(a+1)\geqslant 0,\quad \mathrm{Tr}_{\mathcal{H}_1}[J(1)]=1,\\ &\mathrm{Tr}_{\mathcal{H}_{2i-1}}[J(i)]=\mathrm{Tr}_{\mathcal{H}_{2i-1}\mathcal{H}_{2i-2}}[J(i)]\otimes\mathbb{1}_{\mathcal{H}_{2i-2}},\quad \text{for}\,2\leqslant i\leqslant a+1.\end{aligned} \tag{49}$$

Thus, in this case, we have the following universal uncertainty relation for multiple interactive measurements

$$\bigoplus_{j=1}^b\frac{1}{b}\mathbf{p}_j\prec\mathbf{w}_{\mathcal{T}_1,\ldots,\mathcal{T}_b}. \tag{50}$$

For Shannon entropy H, we obtain

$$\sum_{j=1}^b H(\mathbf{p}_j)\geqslant b\,H(\mathbf{w}_{\mathcal{T}_1,\ldots,\mathcal{T}_b})-b\,\log b, \tag{51}$$

which covers the theorem of our main text. Here the base of logarithms is 2. Moreover, the implementation of the flatness process $\mathcal{F}$ to vector $\mathbf{w}_{\mathcal{T}_1,\ldots,\mathcal{T}_b}$ leads to

$$\bigoplus_{j=1}^b\frac{1}{b}\mathbf{p}_j\prec\mathcal{F}(\mathbf{w}_{\mathcal{T}_1,\ldots,\mathcal{T}_b}), \tag{52}$$

which is optimal under majorization; for any vector $\mathbf{z}$ satisfying $\bigoplus_{j=1}^b\frac{1}{b}\mathbf{p}_j\prec\mathbf{z}$, we have

$$\bigoplus_{j=1}^b\frac{1}{b}\mathbf{p}_j\prec\mathcal{F}(\mathbf{w}_{\mathcal{T}_1,\ldots,\mathcal{T}_b})\prec\mathbf{z}. \tag{53}$$

Thus an improved entropic uncertainty relation can be evaluated as

$$\sum_{j=1}^b H(\mathbf{p}_j)\geqslant b\,H(\mathcal{F}(\mathbf{w}_{\mathcal{T}_1,\ldots,\mathcal{T}_b}))-b\,\log b. \tag{54}$$

Before the end of this section, let us make some remarks. First, the key quantity introduced in Eq. (49) forms a semidefinite program (SDP), which is efficiently computable [14, 15]. Hence, our bound $\sum_{j=1}^b H(\mathbf{p}_j)\geqslant b\,H(\mathcal{F}(\mathbf{w}_{\mathcal{T}_1,\ldots,\mathcal{T}_b}))-b\,\log b$ is also efficiently computable. Second, by taking Bob's quantum dynamics as a quantum state, our result will degenerate into the direct-sum majorization uncertainty relation (without flatness process) introduced in Ref. [16]. There are lots of entropic uncertainty relations [17], but none of them can surpass all the others. In this case, majorization uncertainty relation outperforms other forms of entropic uncertainty relations in a large number of instances, for more details see Refs. [16–18]. Moreover, by taking Bob's quantum dynamics as a quantum channel, our result covers the main result presented in Ref. [11].

III. CAUSAL UNCERTAINTY RELATION

In this section we will prove the Eq. (3) of our main text. Before starting the proof of general result, let us first consider the special case of qubit systems; that is

$$H(\mathcal{T}_{\mathrm{CC}}(U_1,U_2))_{\Phi_{B\to AC}}+H(\mathcal{T}_{\mathrm{DC}}(U_3,U_4))_{\Phi_{B\to AC}}\geqslant 2, \tag{55}$$

with $\mathcal{T}_{\mathrm{CC}}(U_1,U_2)\in\mathcal{M}_{\mathrm{CC}}$ and $\mathcal{T}_{\mathrm{DC}}(U_3,U_4)\in\mathcal{M}_{\mathrm{DC}}$. To identify the dependence and causation, we keep all the subscripts and arguments of interactive measurements in this Supplemental Material. Denote the probability vector obtained from causal map $\Phi_{B\to AC}$ by implementing interactive measurement $\mathcal{T}_{\mathrm{CC}}(U_1,U_2)$ and $\mathcal{T}_{\mathrm{DC}}(U_3,U_4)$ as $\mathbf{p}$ and $\mathbf{q}$ respectively. Here $\mathbf{p}$ is a functional of unitaries U_1, U_2, and causal map $\Phi_{B\to AC}$. Meanwhile, $\mathbf{q}$ is a functional of unitaries U_3, U_4, and causal map $\Phi_{B\to AC}$. According to definition, we have

$$H(\mathcal{T}_{\mathrm{CC}}(U_1,U_2))_{\Phi_{B\to AC}}=H(\mathbf{p}), \tag{56}$$
$$H(\mathcal{T}_{\mathrm{DC}}(U_3,U_4))_{\Phi_{B\to AC}}=H(\mathbf{q}). \tag{57}$$

Let us collect all possible $\mathbf{p}\oplus\mathbf{q}$ together, and denote their collection as $\mathcal{Q}$. For Interactive measurement $\mathcal{T}_{\mathrm{CC}}(U_1,U_2)$, the Choi operator of each effect is given by

$$M_i:=\frac{\mathbb{1}_B}{2}\otimes(U_1^\dagger\otimes U_2^\dagger\left|\Phi_i\right\rangle\!\left\langle\Phi_i\right|U_1\otimes U_2)^{\mathbf{T}},\quad i\in\{1,2,3,4\}. \tag{58}$$

For interactive measurement $\mathcal{T}_{\mathrm{DC}}(U_3,U_4)$, the Choi operator of each effect is described by

$$N_j:=\mathbb{1}_A\otimes(U_3\left|\Phi_1\right\rangle\!\left\langle\Phi_1\right|_{BR}U_3^\dagger)\star(U_4^\dagger\left|\Phi_j\right\rangle\!\left\langle\Phi_j\right|_{CR}U_4)^{\mathbf{T}},\quad j\in\{1,2,3,4\}. \tag{59}$$

Here M_i depends on U_1 and U_2. and the operator N_j depends on U_3 and U_4. Equipped with these notations, let us now start our proof. First, according to the completeness of majorization lattice, there exist a unique least upper bound, denoted as $\vee\mathcal{Q}=(\vee\mathcal{Q}_k)_{k=1}^8$ with $\vee\mathcal{Q}_k\geqslant\vee\mathcal{Q}_{k+1}$ for $1\leqslant k\leqslant 7$, for set $\mathcal{Q}$. Due to the fact that

$$\mathcal{Q}\prec\vee\mathcal{Q}, \tag{60}$$

it is straightforward to check that

$$\vee\mathcal{Q}_1=1, \tag{61}$$
$$\vee\mathcal{Q}_k=0,\quad \text{for } k\geqslant 6. \tag{62}$$

Noted that Eq. (62) comes from the fact that

$$\sum_{k=1}^{5}\vee\mathcal{Q}_k=2. \tag{63}$$

Let us move on to investigating $\vee\mathcal{Q}_2$. From the optimality of $\vee\mathcal{Q}$, we have that

$$\vee\mathcal{Q}_1+\vee\mathcal{Q}_2\leqslant\max_{U_1,\ldots,U_4}\max_{i,j}\max_{\Phi_{B\to AC}}\mathrm{Tr}\big[(M_i+N_j)\cdot J^\Phi\big]. \tag{64}$$

Here the inner maximum is running over all causal maps, and there is no need to consider the summation of operators all coming from $\mathcal{T}_{\mathrm{CC}}(U_1,U_2)$ or $\mathcal{T}_{\mathrm{DC}}(U_3,U_4)$ since in that cases, the summation is less than or equal to 1 (i.e. $\vee\mathcal{Q}_1$). The key point here is the reformulation of the right-hand side of Eq. (64). Writing everything out explicitly, we have

$$\max_{U_1,\ldots,U_4}\max_{i,j}\max_{\Phi_{B\to AC}}\mathrm{Tr}\big[(M_i+N_j)\cdot J^\Phi\big] \tag{65}$$
$$=\max_{U_1,\ldots,U_4}\max_{i,j}\max_{\Phi_{B\to AC}}\mathrm{Tr}\left[(\frac{\mathbb{1}_B}{2}\otimes(U_1^\dagger\otimes U_2^\dagger\left|\Phi_i\right\rangle\!\left\langle\Phi_i\right|U_1\otimes U_2)^{\mathbf{T}}+\mathbb{1}_A\otimes(U_3\left|\Phi_1\right\rangle\!\left\langle\Phi_1\right|_{BR}U_3^\dagger)\star(U_4^\dagger\left|\Phi_j\right\rangle\!\left\langle\Phi_j\right|_{CR}U_4)^{\mathbf{T}})\cdot J^\Phi\right] \tag{66}$$
$$=\max_{U_B}\max_{i,j}\max_{\Phi_{B\to AC}}\mathrm{Tr}\left[((\frac{\mathbb{1}_B}{2}\otimes(\left|\Phi_i\right\rangle\!\left\langle\Phi_i\right|)^{\mathbf{T}}+\mathbb{1}_A\otimes(U_B\left|\Phi_1\right\rangle\!\left\langle\Phi_1\right|_{BR}U_B^\dagger)\star\left|\Phi_j\right\rangle\!\left\langle\Phi_j\right|_{CR}^{\mathbf{T}})\cdot J^\Phi\right] \tag{67}$$
$$=\max_{i,j}\max_{\Phi_{B\to AC}}\mathrm{Tr}\left[((\frac{\mathbb{1}_B}{2}\otimes(\left|\Phi_i\right\rangle\!\left\langle\Phi_i\right|)^{\mathbf{T}}+\mathbb{1}_A\otimes\left|\Phi_1\right\rangle\!\left\langle\Phi_1\right|_{BR}\star\left|\Phi_j\right\rangle\!\left\langle\Phi_j\right|_{CR}^{\mathbf{T}})\cdot J^\Phi\right] \tag{68}$$
$$=5/4, \tag{69}$$

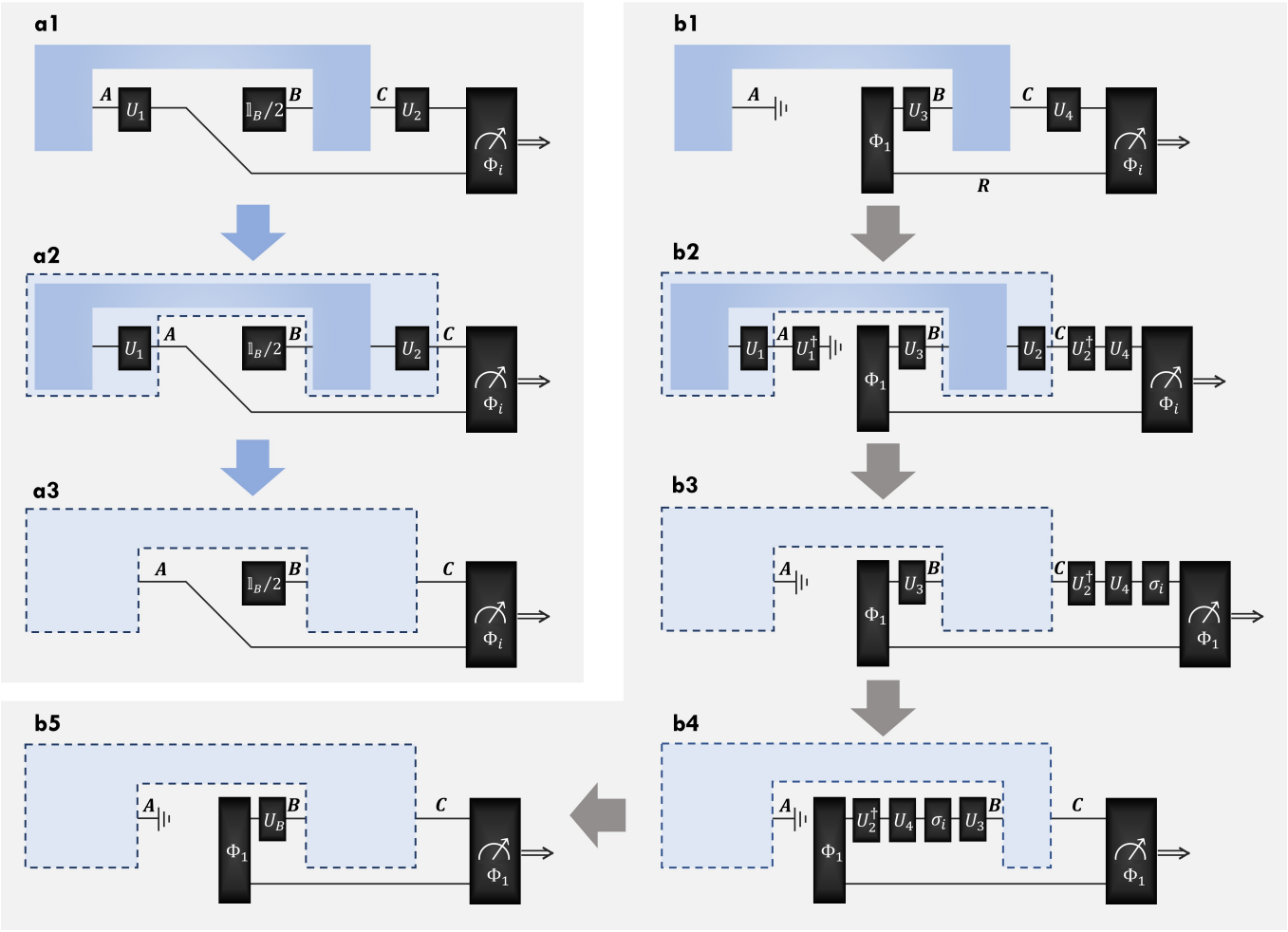

FIG. 3: (color online) Visualization of the process transforming Eq. (66) to Eq. (67). By absorbing U_1 and U_2 into the causal map, we transform the uncertainty relation associated with interactive measurements, illustrated by (a1) and (b1), into the uncertainty relation for (a2) and (b2). As the optimization is taken over all causal maps, we can simply package the quantum dynamics inside the blue dashed box of (a2) and (b2), and reformulate them into (a3) and (b3). The transformation of (b3)→(b4)→(b5) follows directly from the properties of Bell state. Noted that from above visualization, it is clear that Eq. (67) can be further simplified to the following semidefinite programming (SDP) $\max_i \max_{\Phi_{B\to AC}} \mathrm{Tr}\left[\left(\left(\frac{\mathbb{1}_B}{2}\otimes(|\Phi_i\rangle\langle\Phi_i|)\right)^{\mathbf{T}}+\mathbb{1}_A\otimes|\Phi_1\rangle\langle\Phi_1|_{BR}\star|\Phi_1\rangle\langle\Phi_1|^{\mathbf{T}}_{CR}\right)\cdot J^{\Phi}\right]$, whose numerical value is 5/4.

where the second equation is obtained by absorbing unitaries into the causal map (visualized in Fig. 3), and the third equation is a direct consequence of $U_B\,U_B^\dagger=\mathbb{1}$. Finally, the forth equation is the result of SDP formulated in Eq. (68). Therefore, we obtain

$$\vee\mathcal{Q}_1+\vee\mathcal{Q}_2\leqslant 5/4. \tag{70}$$

On the other hand, by choosing $\Phi^{\bullet}_{B\to AC}:=\mathrm{Tr}_E[|\Phi_1\rangle\langle\Phi_1|_{AE}]\otimes\mathrm{id}_{B\to C}$, the corresponding direct-sum of probability vectors become

$$\mathbf{p}^{\bullet}=(1/4,1/4,1/4,1/4), \tag{71}$$
$$\mathbf{q}^{\bullet}=(1,0,0,0). \tag{72}$$

Hence, we have

$$5/4\leqslant\vee\mathcal{Q}_1+\vee\mathcal{Q}_2. \tag{73}$$

Combining Eq. (70) with Eq. (73), we identify that

$$\vee\mathcal{Q}_2=1/4. \tag{74}$$

On the one hand, for the quantities $\vee\mathcal{Q}_k$ $(k=3,4,5)$, if any of them is strictly less than $\vee\mathcal{Q}_2$, then

$$\sum_{k=2}^{5}\vee\mathcal{Q}_k < 4 \vee \mathcal{Q}_2 = 1, \tag{75}$$

and thus

$$\sum_{k}\vee\mathcal{Q}_k < 2, \tag{76}$$

which is a contradiction. On the other hand, according to the definition of $\vee\mathcal{Q}$, $\vee\mathcal{Q}_k$ $(k=3,4,5)$ is upper bounded by $\vee\mathcal{Q}_2$, so that

$$\vee\mathcal{Q}_k = 1/4, \quad \text{for } 2\leqslant k\leqslant 5. \tag{77}$$

It now follows immediately that, for families of infinite unitaries, our universal uncertainty relation for causal maps is given by

$$\mathbf{p}(U_1,U_2)_{\Phi_{B\to AC}}\oplus\mathbf{q}(U_3,U_4)_{\Phi_{B\to AC}}\prec\vee\mathcal{Q}=(1,1/4,1/4,1/4,1/4,0,0,0). \tag{78}$$

This implies that for all unitaries and causal maps,

$$H(\mathcal{T}_{\mathrm{CC}}(U_1,U_2))_{\Phi_{B\to AC}}+H(\mathcal{T}_{\mathrm{DC}}(U_3,U_4))_{\Phi_{B\to AC}}\geqslant H(1/4,1/4,1/4,1/4)=2. \tag{79}$$

Eq. (78) proves that 2 is a bound for $H(\mathcal{T}_{\mathrm{CC}}(U_1,U_2))_{\Phi_{B\to AC}}+H(\mathcal{T}_{\mathrm{DC}}(U_3,U_4))_{\Phi_{B\to AC}}$. Now we further show it is exactly the optimal bound. Actually by taking $\Phi^{\bullet}_{B\to AC}:=\mathrm{Tr}_E[|\Phi_1\rangle\langle\Phi_1|_{AE}]\otimes\mathrm{id}_{B\to C}$ and $U_1=U_2=U_3=U_4=\mathbb{1}$, we have

$$H(\mathcal{T}_{\mathrm{CC}}(\mathbb{1},\mathbb{1}))_{\Phi^{\bullet}_{B\to AC}}+H(\mathcal{T}_{\mathrm{DC}}(\mathbb{1},\mathbb{1}))_{\Phi^{\bullet}_{B\to AC}}=2, \tag{80}$$

which completes the proof.

Actually, above proof for qubit can be extended to the case of qudit straightforwardly by replacing the Pauli operator appeared in Bell measurements and Eq. (71) with Heisenberg-Weyl operators and $(1/d^2,\ldots,1/d^2)$. In particular that, for the case with $\dim A=\dim B=\dim C=d$, we have

$$H(\mathcal{T}_{\mathrm{CC}}(U_1,U_2))_{\Phi_{B\to AC}}+H(\mathcal{T}_{\mathrm{DC}}(U_3,U_4))_{\Phi_{B\to AC}}\geqslant 2\log d, \tag{81}$$

where U_1, U_2, U_3, and U_4 are now d-dimensional unitaries.

IV. QUANTUM CAUSAL INFERENCE

A. Necessary and Sufficient Conditions for Causal Structures

In this section we investigate the model of causal maps again, and provide the necessary and sufficient conditions for a set of causal maps to be direct-cause and common-cause. To start with, let us denote the bipartite quantum channel between systems B and C as $\mathcal{E}_{BE\to CF}$, where we use E and F to represent the environment systems before and after the bipartite unitary. Now a causal map can be written as

$$\Phi_{B\to AC}=\mathrm{Tr}_F[\mathcal{E}_{BE\to CF}(\rho_{AE})], \tag{82}$$

where the environment system F has been deleted. Without loss of generality, we assume that the initial state ρ_{AE} is a pure state, i.e. $\rho_{AE}=\phi_{AE}$, as we can always purify the initial state when the environment system is large enough.

Here we focus on the quantum dynamics $\Phi_{B\to ACF}$ before tracing F (see Fig. 4), which satisfies

$$\mathrm{Tr}_F\circ\Phi_{B\to ACF}=\Phi_{B\to AC}. \tag{83}$$

If the structure of quantum circuit $\Phi_{B\to ACF}$ is *direct-cause*, it has the form

$$\Phi_{B\to ACF}=\rho_{AF}\otimes\mathcal{E}_{B\to C}, \tag{84}$$

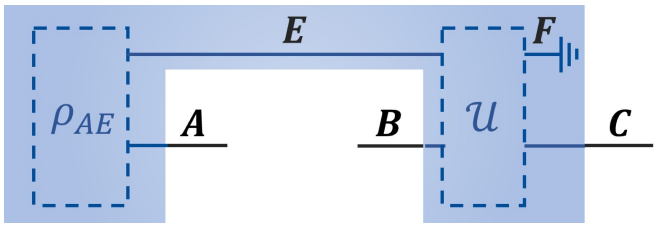

FIG. 4: (color online) Quantum dynamics $\Phi_{B\to ACF}$, where the initial state is ρ_{AE}, and the systems BE and CF are connected through the bipartite unitary $\mathcal{U}_{BE\to CF}$.

where ρ_{AF} is a quantum state on systems AF and $\mathcal{E}_{B\to C}$ is a quantum channel from system B to C. On the other hand, if the structure of quantum circuit $\Phi_{B\to ACF}$ is *common-cause* , it is expressed as

$$\Phi_{B\to ACF} = \rho_{AC} \otimes \mathcal{E}_{B\to F}, \tag{85}$$

where ρ_{AC} is an entangled state on systems AC and $\mathcal{E}_{B\to F}$ is a quantum channel from system B to C.

In this work, we study the case where the bipartite quantum operation $\mathcal{E}_{BE\to CF}$ between BE and CF is a unitary gate; that is

$$\mathcal{E}_{BE\to CF} = \mathcal{U}_{BE\to CF}. \tag{86}$$

In this case, the quantum dynamics $\Phi_{B\to ACF}$ is a pure circuit (namely its Choi operator is pure)

$$\Phi_{B\to ACF} = \mathcal{U}_{BE\to CF}(\phi_{AE}). \tag{87}$$

In particular, if the quantum dynamics $\Phi_{B\to ACF}$ exhibits a direct-cause, we have

$$\mathcal{U}_{BE\to CF}(\phi_{AE}) = \rho_{AF} \otimes \mathcal{E}_{B\to C}. \tag{88}$$

Due to the purity of $\mathcal{U}_{BE\to CF}(\phi_{AE})$, it now follows immediately that ρ_{AF} is a pure state on systems AE and $\mathcal{E}_{B\to C}$ is a unitary gate between systems B and C. Thus, we see that

$$\Phi_{B\to ACF} = \psi_{AF} \otimes \mathcal{U}_{B\to C}, \tag{89}$$

holds for some pure state ψ_{AF} and unitary $\mathcal{U}_{B\to C}$. Hence, in this case, the structure of causal map $\Phi_{B\to AC}$ is direct-cause if and only if

$$H(\mathcal{T}_{\mathrm{DC}}(U_3^\star, U_4^\star))_{\Phi_{B\to AC}} = 0, \tag{90}$$

is satisfied by some unitaries $U_3^\star$ and $U_4^\star$. We now move on to studying the case that $\Phi_{B\to ACF}$ forms a common-cause. As in the above discussion, writing everything out explicitly, we have

$$\mathcal{U}_{BE\to CF}(\phi_{AE}) = \rho_{AC} \otimes \mathcal{E}_{B\to F}. \tag{91}$$

By using the property of purity of $\mathcal{U}_{BE\to CF}(\phi_{AE})$, Eq. (91) can be rewritten as

$$\mathcal{U}_{BE\to CF}(\phi_{AE}) = \psi_{AC} \otimes \mathcal{U}_{B\to F}, \tag{92}$$

with ψ_{AC} being pure state and $\mathcal{U}_{B\to F}$ being unitary gate. Since the input of $\mathcal{U}_{B\to F}$ will not affect the dynamics from E to C, we can further express $\mathcal{U}_{BE\to CF}$ as

$$\mathcal{U}_{BE\to CF} = \mathcal{E}_{E\to C} \otimes \mathcal{U}_{B\to F}, \tag{93}$$

with $\mathcal{E}_{E\to C}$ being a quantum channel from system E to C. Actually, the channel $\mathcal{E}_{E\to C}$ appeared here can only be a unitary. Therefore, in the case that Φ_{AE} is the maximally entangled state, the structure of causal map $\Phi_{B\to AC}$ is common-cause if and only if

$$H(\mathcal{T}_{\mathrm{CC}}(U_1^\star, U_2^\star))_{\Phi_{B\to AC}} = 0, \tag{94}$$

holds for some $U_1^\star$ and $U_2^\star$.

We apply Eq. (3) of main text to infer causal structures. For quantum circuit $\mathrm{Tr}_F[\mathcal{E}_{BE\to CF}(\rho_{AE})]$ with ρ_{AE} being a pure state and $\mathcal{E}_{BE\to CF}$ being a bipartite unitary, if there exists unitaries $U_1^\star$ and $U_2^\star$ such that

$$2 > H(\mathcal{T}_{\mathrm{CC}}(U_1^\star, U_2^\star))_{\Phi_{B\to AC}} > 0, \tag{95}$$

then it follows that

$$H(\mathcal{T}_{\mathrm{DC}}(U_3, U_4))_{\Phi_{B\to AC}} \geqslant 2 - H(\mathcal{T}_{\mathrm{CC}}(U_1^\star, U_2^\star))_{\Phi_{B\to AC}} > 0, \tag{96}$$

for all unitaries U_3 and U_4. Thus, the causal structure of $\Phi_{B\to AC}$ is either common-cause or mixture of both direct-cause and common-cause. In particular, when the initial state ρ_{AE} is the maximally entangled state, then the existence of $U_3^\star$ and $U_4^\star$ such that

$$2 > H(\mathcal{T}_{\mathrm{DC}}(U_3^\star, U_4^\star))_{\Phi_{B\to AC}} > 0, \tag{97}$$

is enough to rule out the possibilities to be common-cause, and thus the corresponding causal structure must be the mixture of both direct-cause and common-cause. In such a scenario, the causal structure is determined by using only two interactive measurements, namely $\mathcal{T}_{\mathrm{CC}}(U_1^\star, U_2^\star)$ and $\mathcal{T}_{\mathrm{DC}}(U_3^\star, U_4^\star)$.

B. Coherent Mixture of Common-Cause and Cause-Effect

We will finish this Supplemental Material by making remarks about the quantum circuit $\Phi_{\alpha,\beta}$ considered in our main text (see also Fig. 5 of our main text). In particular, we will show that $\Phi_{\alpha=-\pi/4,\beta=-\pi/2}$ is a coherent mixture of causal models of common-cause and cause-effect. First, the initially prepared state between system A and environment (hidden system in Fig. 5(a) of the main text) E is the maximally entangled state ϕ_{AE}^+. Remark that all systems considered in $\Phi_{\alpha,\beta}$ are two-level; that is $\dim A = \dim B = \dim C = \dim E = 2$. Second, the bipartite unitary $U(\alpha,\beta)$ from BE to CE is given by

$$U(\alpha,\beta) = e^{i\alpha/2}\begin{pmatrix} e^{-i\alpha} & 0 & 0 & 0 \\ 0 & \cos(\beta/2) & -i\sin(\beta/2) & 0 \\ 0 & -i\sin(\beta/2) & \cos(\beta/2) & 0 \\ 0 & 0 & 0 & e^{-i\alpha} \end{pmatrix}. \tag{98}$$

When $\alpha = -\pi/4$ and $\beta = -\pi/2$, the bipartite unitary $U(\alpha = -\pi/4, \beta = -\pi/2)$ turns out to be

$$U(\alpha = -\pi/4, \beta = -\pi/2) = e^{-i\pi/8}\begin{pmatrix} e^{i\pi/4} & 0 & 0 & 0 \\ 0 & \cos(\pi/4) & i\sin(\pi/4) & 0 \\ 0 & i\sin(\pi/4) & \cos(\pi/4) & 0 \\ 0 & 0 & 0 & e^{i\pi/4} \end{pmatrix}. \tag{99}$$

Thus, written out explicitly, the quantum circuit is

$$\Phi_{\alpha=-\pi/4,\beta=-\pi/2} = \mathrm{Tr}_E[U(\alpha = -\pi/4, \beta = -\pi/2)_{BE\to CE}(\phi_{AE}^+)]. \tag{100}$$

On the other hand, the existence of coherent mixture of causal models of common-cause and cause-effect has been proved by exampling the following quantum circuit $\mathrm{Tr}_E[U_*(\phi_{AE}^+)]$ [13], where

$$U_* = (\cos\pi/4)\mathrm{id}_{B\to C} \otimes \mathrm{id}_{E\to E} + (i\sin\pi/4)\cdot \mathrm{SWAP}(BE \to EC) \tag{101}$$

is the partial swap unitary from BE to CE. More precisely, it is of the form

$$U_* = \begin{pmatrix} e^{i\pi/4} & 0 & 0 & 0 \\ 0 & \cos(\pi/4) & i\sin(\pi/4) & 0 \\ 0 & i\sin(\pi/4) & \cos(\pi/4) & 0 \\ 0 & 0 & 0 & e^{i\pi/4} \end{pmatrix}. \tag{102}$$

It is worth mentioning that for any input state ρ_{BE}, we have

$$U_*\rho_{BE}U_*^\dagger = U(\alpha = -\pi/4, \beta = -\pi/2)\rho_{BE}U(\alpha = -\pi/4, \beta = -\pi/2)^\dagger, \tag{103}$$

which implies that

$$\Phi_{\alpha=-\pi/4,\beta=-\pi/2} = \mathrm{Tr}_E[U_*(\phi_{AE}^+)]. \tag{104}$$

In other words, the quantum circuit $\Phi_{\alpha=-\pi/4,\beta=-\pi/2}$ studied in Fig. 5(c) of the main text is indeed a coherent mixture of both common-cause and cause-effect, which goes beyond the probabilistic mixture of common-cause and cause-effect.

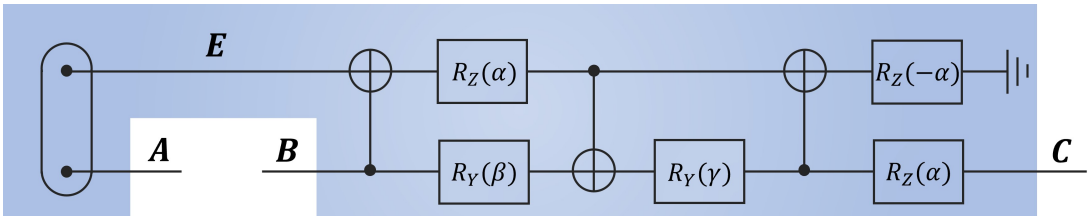

FIG. 5: (color online) Parametrized quantum circuit $\Phi_{\alpha,\beta,\gamma} : B \to AC$, with each parameter controls a Pauli rotation. System A and environment E are initiated in Bell state. Meanwhile, the bipartite evolution from systems B to C is an universal interaction between two qubits [19].

V. NUMERICAL EXPERIMENTS

In the main text of our work, we have demonstrated the numerical experiments for quantum circuit with two parameters. We now move on to illustrating entropic uncertainty relation for quantum circuit with universal bipartite gate between systems B and C, shown in Fig. 5, and further detail how to infer the causal structure associated with quantum circuit based on our framework. We remark that all systems considered in this section are two-level.

A. The Landscape of Joint Uncertainty

As depicted in Fig. 5, here we consider a more general quantum circuit, with system A and environment E are prepared in the Bell state $|\Phi_1\rangle$. The bipartite unitary gate $\mathcal{U}(\alpha,\beta,\gamma)_{BE\to CE}$ between systems B and C constitutes of three CNOT gates and five Pauli rotations. More precisely, the rotation gates with respect to z and y axis are defined as

$$R_z(\theta) := \begin{pmatrix} e^{-i\theta/2} & 0 \\ 0 & e^{i\theta/2} \end{pmatrix}, \quad R_y(\theta) := \begin{pmatrix} \cos(\theta/2) & -\sin(\theta/2) \\ \sin(\theta/2) & \cos(\theta/2) \end{pmatrix} . \tag{105}$$

Here $\mathcal{U}(\alpha,\beta,\gamma)_{BE\to CE}$ is a family of universal two-qubit unitary gates, up to some local unitary pre- and post-operations [19]. Since the system E is traced out at the end, the post-operation on system E can be discarded. As the dynamics is initiated in a Bell state, any unitary pre-operation on system E is equivalent to its transpose acting on system A. Consequently, this family of two-qubit unitary operators are universal up to some local unitary operator on system A, B and C. The two R_z gates at the end are inserted merely for aesthetic purposes. Now the whole family of quantum circuits is given by the following quantum dynamics

$$\Phi_{\alpha,\beta,\gamma} := \mathrm{Tr}_E[\mathcal{U}(\alpha,\beta,\gamma)_{BE\to CE}(|\Phi_1\rangle\langle\Phi_1|)]. \tag{106}$$

Our numerical experiments are plotted at different values of γ, and runs over α and β each from $-\pi$ to π. The values of joint uncertainty for interactive measurements $\mathcal{T}_{\mathrm{CC}}(\mathbb{1},\mathbb{1})$ and $\mathcal{T}_{\mathrm{DC}}(\mathbb{1},\mathbb{1})$, namely

$$H(\mathcal{T}_{\mathrm{CC}}(\mathbb{1},\mathbb{1}))_{\Phi_{\alpha,\beta,\gamma}} + H(\mathcal{T}_{\mathrm{DC}}(\mathbb{1},\mathbb{1}))_{\Phi_{\alpha,\beta,\gamma}}, \tag{107}$$

with respect to quantum circuits $\Phi_{\alpha,\beta,\gamma}$ and our bound 2 are compared in Fig. 6, which shows the tightness of our bound.

B. Advantage in Inferring Causal Structure

In this section, we investigate the causal structure associated with parametrized quantum circuit $\Phi_{\alpha,\beta,\gamma}$ (see Fig. 5) by using our framework. Recall that in this case, where the systems between A and E are maximally entangled state and the quantum channel from BE to CE is a bipartite unitary gate, the circuit reveals a direct-cause if and only if

$$H(\mathcal{T}_{\mathrm{DC}}(U_3^\star, U_4^\star))_{\Phi_{\alpha,\beta,\gamma}} = 0, \tag{108}$$

is satisfied by some unitaries $U_3^\star$ and $U_4^\star$. On the other hand, the circuit contains a common-cause if and only if the equation

$$H(\mathcal{T}_{\mathrm{CC}}(U_1^\star, U_2^\star))_{\Phi_{\alpha,\beta,\gamma}} = 0, \tag{109}$$

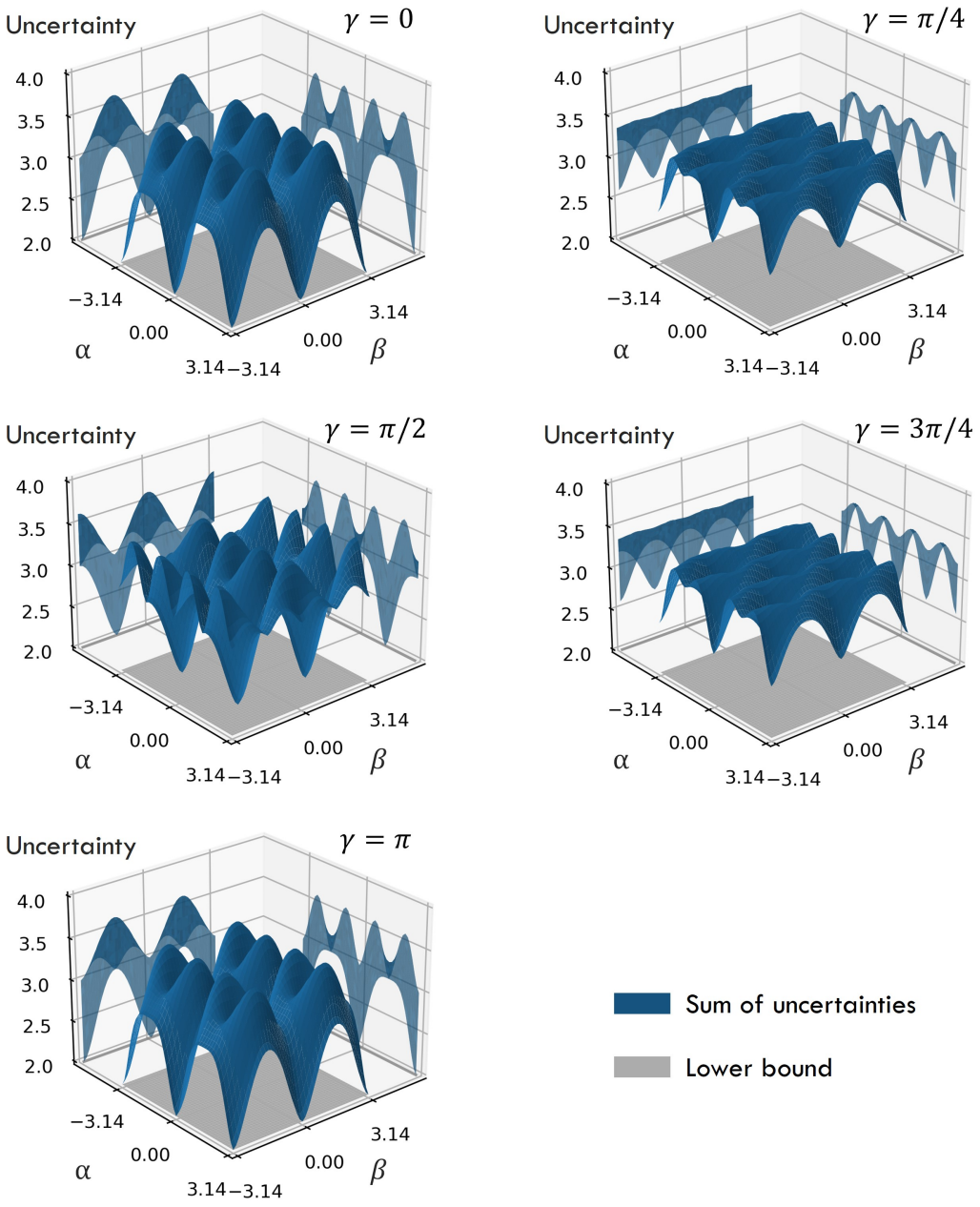

FIG. 6: (color online) Comparison between the joint uncertainties $H(\mathcal{T}_{\mathrm{CC}}(\mathbb{1},\mathbb{1}))_{\Phi_{\alpha,\beta,\gamma}} + H(\mathcal{T}_{\mathrm{DC}}(\mathbb{1},\mathbb{1}))_{\Phi_{\alpha,\beta,\gamma}}$ (blue) and our bound 2 (gray) with different parameters.

holds for some $U_1^\star$ and $U_2^\star$.

Here we have depicted the Shannon entropy of $H(\mathcal{T}_{\mathrm{CC}}(\mathbb{1},\mathbb{1}))_{\Phi_{\alpha,\beta,\gamma}}$ and $H(\mathcal{T}_{\mathrm{DC}}(\mathbb{1},\mathbb{1}))_{\Phi_{\alpha,\beta,\gamma}}$ in Fig. 7. For parameters $\alpha^\star$, $\beta^\star$ and $\gamma^\star$, if $H(\mathcal{T}_{\mathrm{CC}}(\mathbb{1},\mathbb{1}))_{\Phi_{\alpha^\star,\beta^\star,\gamma^\star}} \in (0,2)$, the entropy $H(\mathcal{T}_{\mathrm{DC}}(U_3,U_4))_{\Phi_{\alpha^\star,\beta^\star,\gamma^\star}}$ satisfies the following inequality,

$$H(\mathcal{T}_{\mathrm{DC}}(U_3,U_4))_{\Phi_{\alpha^\star,\beta^\star,\gamma^\star}} \geqslant 2 - H(\mathcal{T}_{\mathrm{CC}}(\mathbb{1},\mathbb{1}))_{\Phi_{\alpha^\star,\beta^\star,\gamma^\star}} > 0, \tag{110}$$

for all U_3 and U_4. Thus, the causal structure of circuit $\Phi_{\alpha^\star,\beta^\star,\gamma^\star}$ will never be direct-causal. Meanwhile, for the same parameters $\alpha^\star$, $\beta^\star$ and $\gamma^\star$, if $H(\mathcal{T}_{\mathrm{DC}}(\mathbb{1},\mathbb{1}))_{\Phi_{\alpha^\star,\beta^\star,\gamma^\star}} \in (0,2)$, then we have

$$H(\mathcal{T}_{\mathrm{CC}}(U_1,U_2))_{\Phi_{\alpha^\star,\beta^\star,\gamma^\star}} \geqslant 2 - H(\mathcal{T}_{\mathrm{DC}}(\mathbb{1},\mathbb{1}))_{\Phi_{\alpha^\star,\beta^\star,\gamma^\star}} > 0, \tag{111}$$

for all U_1 and U_2. Hence, the causal structure of $\Phi_{\alpha^\star,\beta^\star,\gamma^\star}$ cannot be common-cause.

To summarize, for the parametrized quantum circuit $\Phi_{\alpha^\star,\beta^\star,\gamma^\star}$, if the numerical value of Shannon entropies $H(\mathcal{T}_{\rm CC}(\mathbb{1},\mathbb{1}))_{\Phi_{\alpha^\star,\beta^\star,\gamma^\star}}$ and $H(\mathcal{T}_{\rm DC}(\mathbb{1},\mathbb{1}))_{\Phi_{\alpha^\star,\beta^\star,\gamma^\star}}$ belongs to $(0,2)$, the corresponding causal structure must be a mixture of both direct-cause and common-cause. The real surprise is that such a deterministic statement about causal structure of $\Phi_{\alpha^\star,\beta^\star,\gamma^\star}$ is obtained by implementing only two interactive measurements, which outperforms the standard approach of causal tomography.

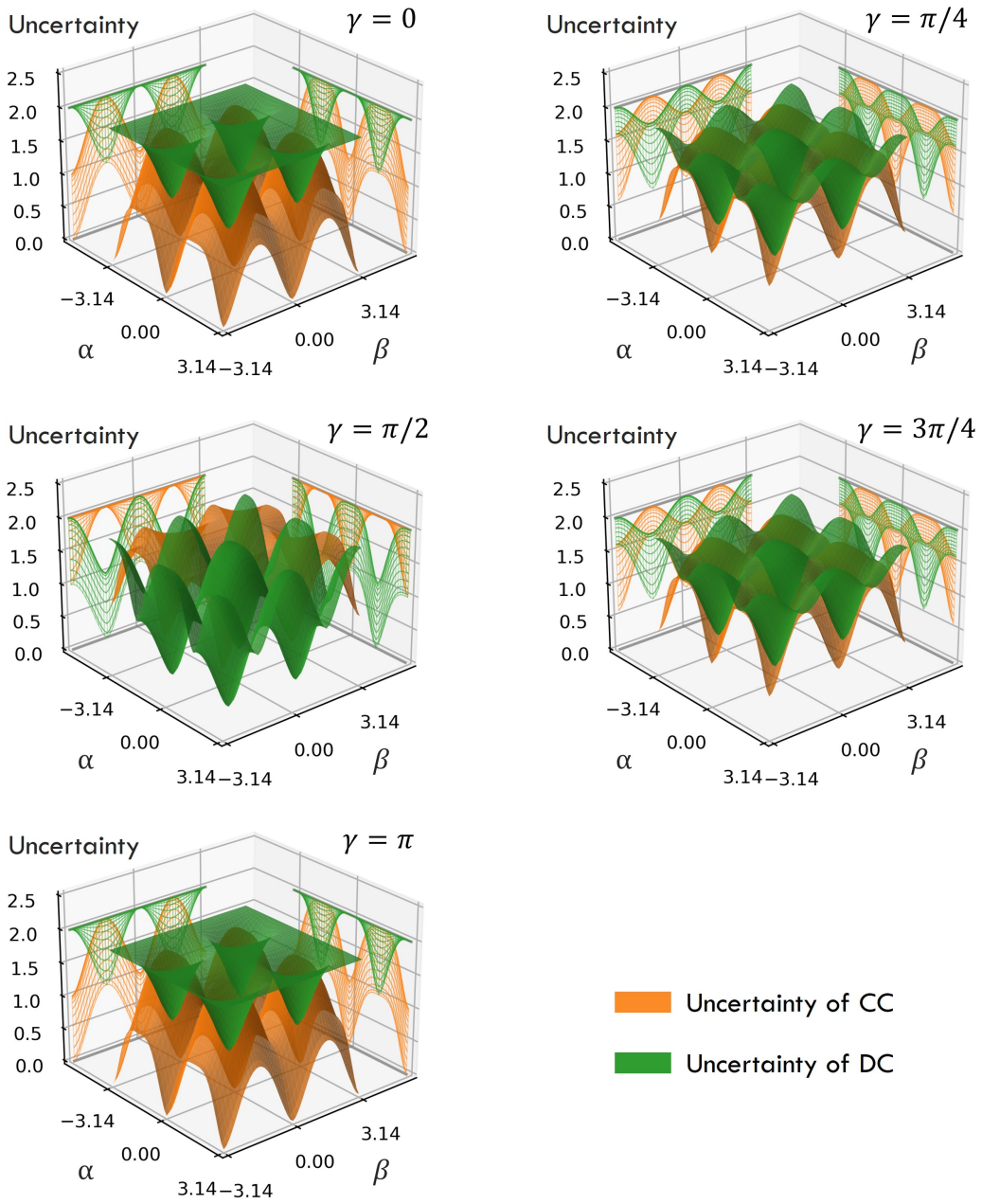

FIG. 7: (color online) Illustration of the Shannon entropies $H(\mathcal{T}_{\rm CC}(\mathbb{1},\mathbb{1}))_{\Phi_{\alpha,\beta,\gamma}}$ (yellow) and $H(\mathcal{T}_{\rm DC}(\mathbb{1},\mathbb{1}))_{\Phi_{\alpha,\beta,\gamma}}$ (green) with different parameters. If the numerical value of $H(\mathcal{T}_{\rm CC}(\mathbb{1},\mathbb{1}))_{\Phi_{\alpha^\star,\beta^\star,\gamma^\star}}$ falls into the interval of $(0,2)$ for some $(\alpha^\star,\beta^\star,\gamma^\star)$, then the circuit $\Phi_{\alpha^\star,\beta^\star,\gamma^\star}$ cannot reveal a direct-cause. Meanwhile, if $H(\mathcal{T}_{\rm DC}(\mathbb{1},\mathbb{1}))_{\Phi_{\alpha^\star,\beta^\star,\gamma^\star}}$ falls into the interval of $(0,2)$ for some $(\alpha^\star,\beta^\star,\gamma^\star)$, the causal structure of $\Phi_{\alpha^\star,\beta^\star,\gamma^\star}$ is not common-cause. If both $H(\mathcal{T}_{\rm CC}(\mathbb{1},\mathbb{1}))_{\Phi_{\alpha^\star,\beta^\star,\gamma^\star}}$ and $H(\mathcal{T}_{\rm DC}(\mathbb{1},\mathbb{1}))_{\Phi_{\alpha^\star,\beta^\star,\gamma^\star}}$ belongs to $(0,2)$ for some $(\alpha^\star,\beta^\star,\gamma^\star)$, the causal structure of quantum circuit $\Phi_{\alpha^\star,\beta^\star,\gamma^\star}$ exhibits a mixture of both direct-cause and common-cause.

For the case $\beta=\gamma$, we have demonstrated all the circuits whose causal structure can be obtained by implementing only two interactive measurements in Fig. 8, where the green (dashed) line stands for the uncertainty associated with

$\mathcal{T}_{\mathrm{DC}}(\mathbb{1},\mathbb{1})$ and the yellow (dashed) line represents the uncertainty associated with $\mathcal{T}_{\mathrm{CC}}(\mathbb{1},\mathbb{1})$. In particular, the dashed lines stand for the case when the uncertainty is equal to 2, where we cannot get any useful information about the causal structure of $\Phi_{\alpha,\beta,\gamma}$. The dots stand for the case whose uncertainty is equal to 0. For these dots, we can get a deterministic statement about its causal structure. Take the green (yellow) dots for instance, the causal structure of circuit $\Phi_{\alpha,\beta,\beta}$ is direct-cause (common-cause). It is clear from our examples (i.e. $\Phi_{\alpha,\beta,\beta}$) that the causal structure of almost all circuits can be determined by using only two interactive measurements.

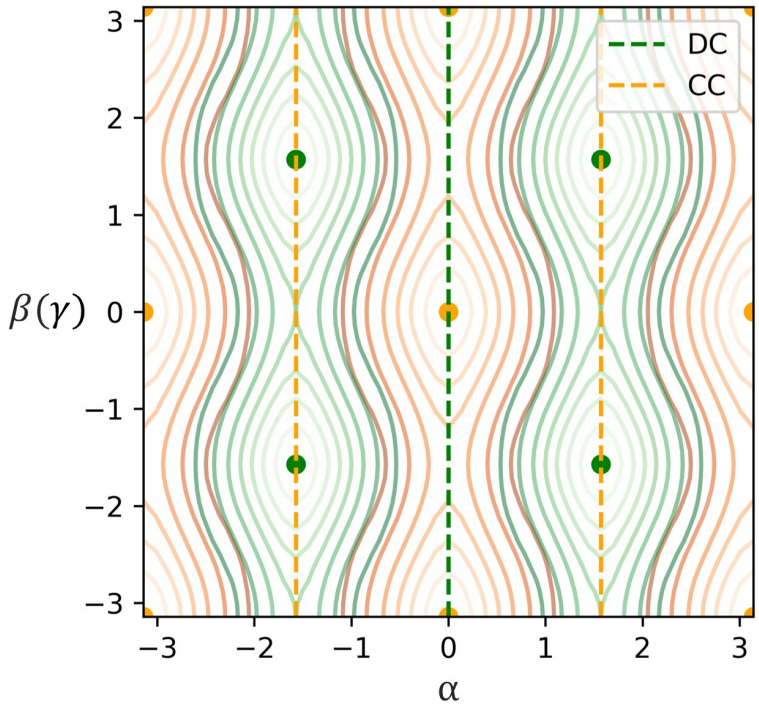

FIG. 8: (color online) Contour lines for the uncertainty associated with interactive measurements $\mathcal{T}_{\mathrm{DC}}(\mathbb{1},\mathbb{1})$ and $\mathcal{T}_{\mathrm{CC}}(\mathbb{1},\mathbb{1})$. Here the green dashed line stand for the cases where $H(\mathcal{T}_{\mathrm{DC}}(\mathbb{1},\mathbb{1}))_{\Phi_{\alpha,\beta,\beta}} = 2$, and the yellow dashed line represents the cases where $H(\mathcal{T}_{\mathrm{CC}}(\mathbb{1},\mathbb{1}))_{\Phi_{\alpha,\beta,\beta}} = 2$. The green and yellow dots are the tuples (α,β) such that $H(\mathcal{T}_{\mathrm{DC}}(\mathbb{1},\mathbb{1}))_{\Phi_{\alpha,\beta,\beta}} = 0$ and $H(\mathcal{T}_{\mathrm{CC}}(\mathbb{1},\mathbb{1}))_{\Phi_{\alpha,\beta,\beta}} = 0$. In such cases, the corresponding causal structures are direct-cause and common-cause respectively. Besides dashed lines and dotted, all other quantum circuits exhibit a mixture of both direct-cause and common-cause.

[1] A. Jamiołkowski, Linear transformations which preserve trace and positive semidefiniteness of operators, Reports on Mathematical Physics **3**, 275 (1972).
[2] M.-D. Choi, Completely positive linear maps on complex matrices, Linear Algebra and its Applications **10**, 285 (1975).
[3] M. A. Nielsen and I. L. Chuang, *Quantum Computation and Quantum Information: 10th Anniversary Edition* (Cambridge University Press, 2010).
[4] M. M. Wilde, *Quantum Information Theory* (Cambridge University Press, 2013).
[5] J. Watrous, *The Theory of Quantum Information* (Cambridge University Press, 2018).
[6] G. Chiribella, G. M. D'Ariano, and P. Perinotti, Quantum circuit architecture, Phys. Rev. Lett. **101**, 060401 (2008).
[7] G. Chiribella, G. M. D'Ariano, and P. Perinotti, Theoretical framework for quantum networks, Phys. Rev. A **80**, 022339 (2009).
[8] G. Chiribella, G. M. D'Ariano, and P. Perinotti, Transforming quantum operations: Quantum supermaps, EPL **83**, 30004 (2008).
[9] F. Cicalese and U. Vaccaro, Supermodularity and subadditivity properties of the entropy on the majorization lattice, IEEE Transactions on Information Theory **48**, 933 (2002).
[10] A. Marshall, I. Olkin, and B. Arnold, *Inequalities: Theory of Majorization and Its Applications*, Springer Series in Statistics (Springer New York, 2010).

[11] Y. Xiao, K. Sengupta, S. Yang, and G. Gour, Uncertainty principle of quantum processes, Phys. Rev. Research **3**, 023077 (2021).
[12] K. Ried, M. Agnew, L. Vermeyden, D. Janzing, R. W. Spekkens, and K. J. Resch, A quantum advantage for inferring causal structure, Nature Physics **11**, 414 (2015).
[13] J.-P. W. MacLean, K. Ried, R. W. Spekkens, and K. J. Resch, Quantum-coherent mixtures of causal relations, Nature Communications **8**, 15149 (2017).
[14] L. Vandenberghe and S. Boyd, Semidefinite programming, SIAM Review **38**, 49 (1996), https://doi.org/10.1137/1038003.
[15] S. Boyd and L. Vandenberghe, *Convex Optimization* (Cambridge University Press, 2004).
[16] L. Rudnicki, Z. Puchała, and K. Życzkowski, Strong majorization entropic uncertainty relations, Phys. Rev. A **89**, 052115 (2014).
[17] P. J. Coles, M. Berta, M. Tomamichel, and S. Wehner, Entropic uncertainty relations and their applications, Rev. Mod. Phys. **89**, 015002 (2017).
[18] S. Friedland, V. Gheorghiu, and G. Gour, Universal uncertainty relations, Phys. Rev. Lett. **111**, 230401 (2013).
[19] V. V. Shende, I. L. Markov, and S. S. Bullock, Minimal universal two-qubit controlled-not-based circuits, Phys. Rev. A **69**, 062321 (2004).